

“Distorted” (η^6 -Arene)tricarbonylchromium Complexes: Correlation of Structural Parameters with the Electronegativity χ_G and Hammett Constants σ_p of Arene Substituents

Jean-Pierre Djukic,^{*,[a]} Françoise Rose-Munch,^[b] Eric Rose,^{*,[b]} and Jacqueline Vaissermann^[c]

Keywords: Substituent effect / Carbonyl complexes / Chromium / Arene complexes / Structure-activity relationships

The molecular structures of 34 (η^6 -arene)tricarbonylchromium complexes have been retrieved from the Cambridge Structural Data Base and investigated by focusing essentially on the distortions of the arene ligand caused by the electronic properties of the substituents connected to it. Two additional *meta*-disubstituted and one *ortho*-disubstituted arene complexes have been synthesized and their structure established by X-ray diffraction analysis. Two types of geometrical parameters have been chosen. The first one is the deviation Δ_i of the value of the endocyclic angle α_i at carbon *ipso* with respect to the ideal value α_0 . The second one encompasses the chromium to *ipso*-carbon and the chromium to ring distances, d_{ipso} and d_0 respectively. It is shown that as long as no reson-

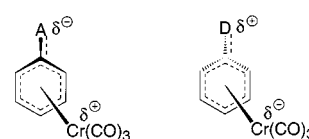
ance effects interfere, Δ_i correlates with the group electronegativity for a wide variety of substituents whose central atom belongs to the first, second or even the third row of the periodic table. Similarly, we find that for mono-substituted arene complexes, d_{ipso} as well as d_0 correlate with the Hammett constants σ_p and σ_p^+ . It is further evident that for a large variety of mono- and di-substituted (η^6 -arene)tricarbonylchromium complexes, d_{ipso} correlates linearly with the σ_p^+ constant, thus indicating that d_{ipso} is a specific geometric constraint imposed by the electronic properties (e.g. inductive and mesomeric) of a given substituent connected to the arene ligand.

Introduction

The outstanding potential that (η^6 -arene)tricarbonylchromium complexes bring to metal-mediated syntheses stems essentially from the stereochemical and electron-withdrawing properties of the $\text{Cr}(\text{CO})_3$ moiety.^[1] This has naturally led many groups of researchers to consider the $\text{Cr}(\text{CO})_3$ moiety as a particularly electrophilic group which could activate a coordinated aromatic ligand toward many types of reactions that would otherwise not be feasible. It is well established that the conformational behavior of the $\text{Cr}(\text{CO})_3$ moiety is controlled by two main parameters: first, the electronic intrinsic properties of the substituents of the arene ring and, second the steric interactions of the substituents with the metal centered rotor.^[2] In the absence of any perturbing bulky group, it may be expected that electron-donating groups will favor a *syn*-eclipsed conformation of $\text{Cr}(\text{CO})_3$ while electron-withdrawing groups will induce an *anti*-eclipsed conformation. In the solid state, the $\text{Cr}(\text{CO})_3$ unit frequently adopts the theoretically predicted conformation although some exceptions suggest that crystal packing may impose unexpected geometries.

In a series of reports,^[3] Hunter and co-workers underlined the peculiar strong distortion of complexed aromatic

rings caused by π -donor substituents such as $-\text{NR}_2$. The authors investigated the possible relationship between the π -donating or π -accepting capability of a given group and the amplitude of the distortions operating over the aromatic ligand, and proposed in some cases that a π -accepting substituent **A** would induce a bending of the aromatic *ipso* carbon toward the $\text{Cr}(\text{CO})_3$ moiety while the opposite would be observed with a π -donating substituent **D**^[3a] (Scheme 1).



Scheme 1

This empirical model was proposed without fully considering the fact that the distortions induced by π -accepting substituents (e.g. out of mean-plane folding of the arene ring toward Cr) were quite rare and small. Relevant distortions of the mean-plane in the vicinity of C_{ipso} may generally be observed only with derivatives of aniline. Therefore we decided to reinvestigate the matter by systematically analyzing the molecular structures of mono-substituted and *para*-, *meta*- and *ortho*-disubstituted (η^6 -arene) $\text{Cr}(\text{CO})_3$ complexes for their main structural properties. This was done by focusing on a set of selected structural parameters that are likely to vary depending exclusively on the electronic effects of the substituent. We show, herein, in an unprecedented manner, that these structural parameters can be correlated in a ma-

[a] UMR 7513 CNRS, Université Louis Pasteur, 4, rue Blaise Pascal, 67070 Strasbourg Cedex, France
E-mail: djukic@chimie.u-strasbg.fr

[b] UMR 7611 CNRS, Université Pierre et Marie Curie, Case 181, 4, place Jussieu, 75252 Paris Cedex 05, France
E-mail: rose@ccr.jussieu.fr

[c] ESA 7071 CNRS, Université Pierre et Marie Curie 4, place Jussieu, 75252 Paris Cedex 05, France

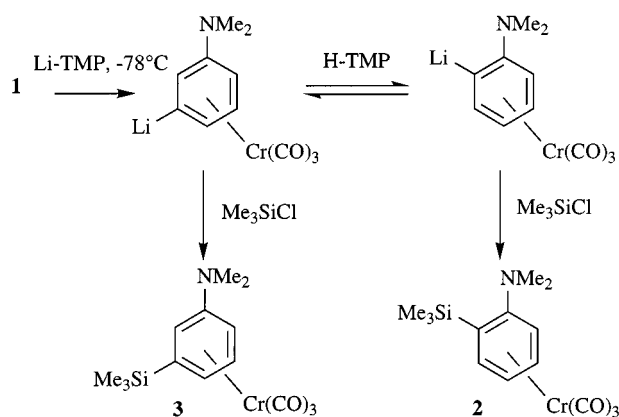
jority of cases to the Hammett constants σ_p , σ_p^+ , to a lesser extent to σ_p^- and to the group electronegativity χ_G of a given substituent $-G$, hence allowing further empirical predictions of the structure-reactivity features of any (η^6 -arene)Cr(CO)₃ complex.

Results and Discussion

For this study, we have investigated a total of 33 X-ray structures and 1 neutron diffraction structure deposited with the Cambridge Structural Data Base (CSDb). Among these, 17 are structures of mono-substituted arene complexes, 13 are of *para*-disubstituted arene complexes and 3 are of hetero-*ortho*-disubstituted arene complexes. We have synthesized three additional complexes, two *meta*-, and one *ortho*- hetero-disubstituted arene complexes, **3**, **4**, and **5**, respectively.

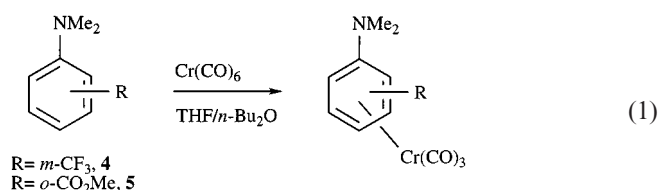
Preparation of Complexes 3–5

Preparation of complex **3** was performed by sequential lithiation and silylation of **1**, (η^6 -NMe₂-C₆H₅)Cr(CO)₃ (Scheme 2). The use of *n*BuLi as a lithiation agent afforded, after silylation, a mixture of complexes **2** and **3**^[4] in a ratio of 46:54, respectively (48% overall yield). In order to optimize the yield of complex **3** we used another method of lithiation first proposed by Kündig and co-workers for (η^6 -naphthalene)tricarbonylchromium.^[5] 1-Lithio-2,2,6,6-tetramethylpiperidine (Li-TMP) reacted with **1** and Me₃SiCl. Complexes **2** and **3** were obtained in a ratio of 21:79 (72% overall yield). In addition, we noticed that a slight excess of 2,2,6,6-tetramethylpiperidine (H-TMP) in the basic reaction medium could cause the formation of a 50:50 mixture of complexes **2** and **3** after silylation (63% overall yield).



Scheme 2

Complex **4** was prepared by the usual method of thermolysis of Cr(CO)₆ in a THF/*n*Bu₂O mixture in the presence of 1-dimethylamino-3-trifluoromethylbenzene [Equation (1)].^[6] Complex **5** was obtained in a similar manner to complex **4**, by thermolysis of Cr(CO)₆ in presence of methyl 2-(dimethylamino)benzoate (Equation 1).



The bright orange complex was purified by the usual techniques and crystallized from a toluene/hexane solution. Single crystals of compounds **3–5** were analyzed by X-ray diffraction. It is worthy to note that the crystal system of compound **3** was found to fit the noncentrosymmetric space group *P*2₁2₁2₁, thus indicating that complex **3** afforded, upon crystallization, a conglomerate^[7] of spontaneously resolved enantiomers (Figure 1). Acquisition and refinement data for **3–5** are provided in Table 7 in the Experimental section of this paper. Selected interatomic distances and valence angles for compounds **3–5** are given in Table 1. Figures 1–3 display ORTEP diagrams and the atom numbering scheme for these three complexes. The three molecular structures display a significant shift of the *ipso* carbon bearing the $-NMe_2$ substituent, out of the mean-aromatic plane away from the Cr center. Compound **5** possesses a pronounced helicity due to both the distortion induced by the $-NMe_2$ group and the *ortho* relationship between the two arene substituents from which steric repulsions arise (Figure 3). The latter helicity is characterized by an absolute value of the torsion angle N–C1–C2–C9 of 15.2°.

Selection of the Structural Parameters Investigated

Although all the structures that were analyzed presented distortions of various parameters such as interatomic distances, valence angles, torsion angles, along with some unexpected conformations of the tripod, we decided to focus essentially on the variation of two elementary parameters that were expected to be sensitive to relatively independent effects. Thus, we somewhat aimed at a rationalization of the causes of arene ligand distortions through a decomposition of the overall phenomenon into a sum of independent contributions. Hence, the following parameters were selected:

1. the deviations Δ_i of the endocyclic angles α_i from the ideal α_0 value of 120.0°,

$\Delta_i = \alpha_i - \alpha_0$, and especially the one centered at C_{ipso} , e.g. Δ_{ipso} (Scheme 3).

2. the chromium to C_{ipso} interatomic distance, d_{ipso} , and the distance from the Cr atom to the mean-aromatic plane, d_0 (Scheme 4).

To justify the study of the endocyclic angle, it must be recalled that with uncoordinated aromatics it is well established that the electronegativity χ_G of a given substituent $-G$ affects the values of both the six endocyclic angles and the corresponding intracyclic $C_{Ar}-C_{Ar}$ bond lengths.^[8] Several studies have shown that a linear correlation between Δ_{ipso} and χ_G , the electronegativity of the group or element,

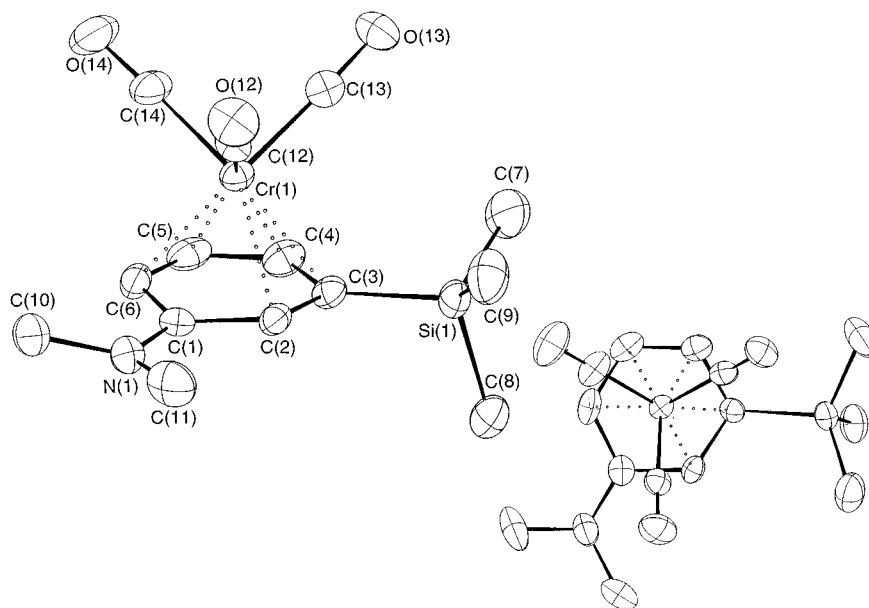


Figure 1. ORTEP diagrams and atomic numbering scheme of the molecular structure of complex **3** including a view along the Cr-ring axis

Table 1. Selected interatomic distances (Å) and valence angles (deg) for compounds **3–5**

compounds	3	4	5
interatomic distances (Å)			
Cr–C1	2.348(7)	2.41(1)	2.383(3)
Cr–C2			2.232(3)
Cr–C3	2.247(7)	2.170(1)	
Cr–C _{Ar} (aver.)	2.244	2.245	2.240
C1–C2	1.431(8)	1.39(1)	1.434(4)
C _{Ar} –C _{Ar} (aver.)	1.41	1.40	1.40
C1–N	1.355(9)	1.37(1)	1.362(4)
C3–SiMe ₃	1.870(6)		
C3–CF ₃		1.48(1)	
C2–CO ₂ Me			1.505(4)
angles of valence (deg)			
C6–C1–C2	115.6(6)	117.6(9)	116.6(3)
C3–C4–C5	120.2(6)	117.1(8)	118.9(3)
C2–C3–C4	117.2(6)	121.3(8)	121.9(3)

may be obtained provided that the central atom of the substituent -G connected to the arene ring belongs to the second or third row of the periodic table and/or does not show propensity to conjugate a doublet of electrons with the π -system of the considered aromatic.^[9] A rationalization of the distortion of α_{ipso} by the VSEPR theory has been proposed: a σ -electron-withdrawing substituent polarizes the localized C_{ipso} -G bonding molecular orbital, so that the bonding electron pair occupies less space in the valence shell of carbon and interacts less strongly with the two neighboring C_{ipso} - C_{ortho} σ -bonding pairs; this causes an increase in the actual value of the internal angle α_{ipso} with respect to the value α_0 , greater than that expected for a substituent having the same electronegativity as the ring; the reverse is expected with a σ -donating substituent. It has been further

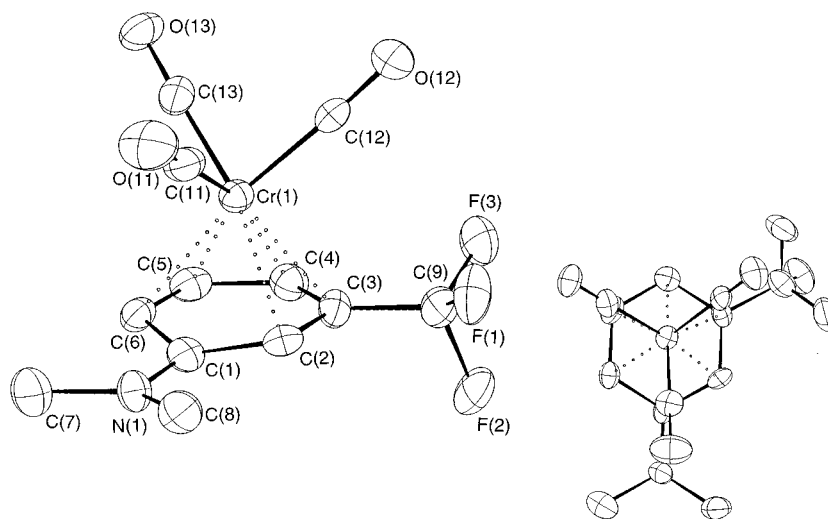


Figure 2. ORTEP diagrams and atomic numbering scheme of the molecular structure of complex **4** including a view along the Cr-ring axis

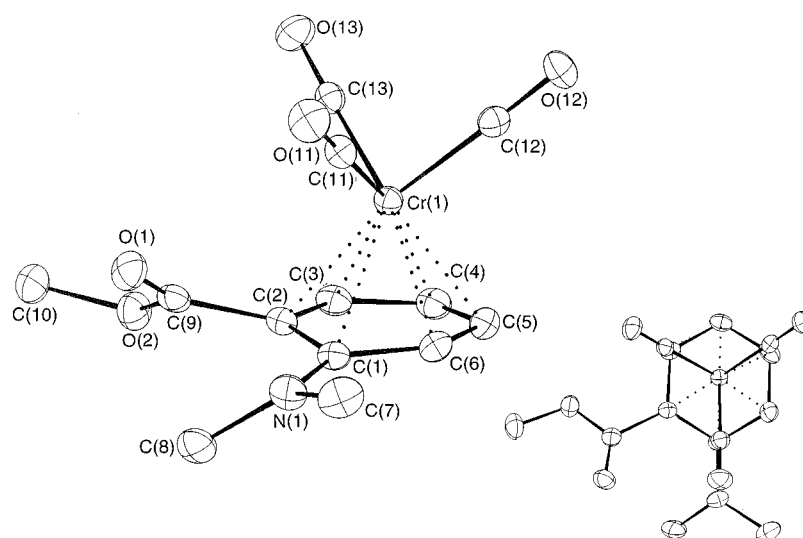
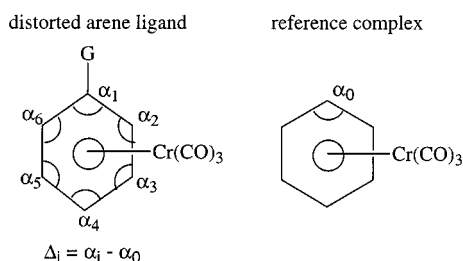
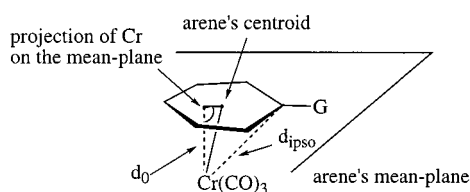


Figure 3. ORTEP diagrams and atomic numbering scheme of the molecular structure of complex **5** including a view along the Cr–ring axis



Scheme 3



Scheme 4

stressed that *if the substituent is conjugated with the ring, there is a build-up of π -electron density alongside the σ -bond and an increase of electron density within the σ -bonding molecular orbital*, in the region of the C_{ipso} –G bond, causing a decrease in the value of α_{ipso} below that of α_0 . Similar trends can be expected for aromatic ligands coordinated to a $Cr(CO)_3$ moiety as it is often the π orbitals of the aromatic fragment that are involved in the interaction with molecular orbitals of $Cr(CO)_3$. The main results of the first part of our investigations are presented in the following paragraph. A preliminary and similar approach has recently been applied to a few examples of metallated (η^6 -arene) $Cr(CO)_3$ σ - π complexes by Lotz and co-workers.^[10]

Our interest in the study of the variation of metal-to-ring distances arose from the numerous comparative studies of the IR spectroscopic properties of substituted arene complexes. They concluded, in a convergent manner, that both

the resonance and inductive electronic effects of the substituent can be readily transmitted to the CO ligands *via* the chromium center.^[11] This has been shown by a net correlation between Hammett σ constants and the force constant k_{CO} of the studied carbonyl ligand C–O bond. This important fact suggested that the arene carbon σ -framework participates in the metal–ring bonding, although the metal-3d and $4p_\pi$ /arene- $2p_\pi$ interaction dominates.^[12] Early semi-empirical molecular orbital calculations carried out by Carroll and McGlynn^[13] pointed out the importance of the ring σ -framework in the arene–Cr bonding. Recently, Phillips and co-workers studied the charge distribution in a series of poly-methyl-substituted (η^6 -benzene) $Cr(CO)_3$ derivatives. They noted that with increasing methyl substitution, the major electron reorganization occurs in the arene–Cr segment of the molecule.^[14] This reorganization, caused by an increase of the degree of substitution of the arene ring by methyl groups, was shown to induce an increase in the arene–Cr bond charge and order. Furthermore, it showed a progressive displacement of the bond charge from the arene ligand toward the chromium atom.

While retrieving the X-ray diffraction structural information of a large series of complexes we noticed that severe foldings of the arene ring away from the $Cr(CO)_3$ group were mostly occurring in aniline derivatives bearing $-NR_2$ groups. In a few examples, other π -electron donating or accepting substituents seemed to induce a significant folding of the ring. However, the main trend observed for complexes bearing π/σ -donor and π/σ -acceptor substituents was an increase and a decrease, respectively, in the chromium-to-*ipso*-carbon distance relative to the reference compound (η^6 -benzene) $Cr(CO)_3$. This general trend somewhat rectifies and refines the empirical rule formulated by Hunter and co-workers and suggests that a folding of the arene ring is generally not necessary for the minimization of intramolecular electronic repulsions, especially in complexes bearing π -donor/acceptor substituents.

Table 2. Endocyclic angular deviations (deg) for mono-substituted arene complexes bearing a substituent -G with an electronegativity of χ_G

entry	-G compound	Δ_1 (deg)	Δ_2 (deg)	Δ_3 (deg)	Δ_4 (deg)	Δ_5 (deg)	Δ_6 (deg)	$\Sigma\Delta_i$ (deg)	$\sigma(\alpha)$ averaged	χ_G
1	-C(O)Me, 6a	0.98	-2.24	4.93	-2.32	-2.32	-0.42	-0.29	—	2.864
2	-H, 6b	0.0	0.0	0.0	0.0	0.0	0.0	0.0	0.09	2.176
3	-NEt ₂ , 6c	-3.4	1.3	0.8	-1.5	2.2	-0.1	-0.7	0.3	3.011
4	-AsPh ₂ , 6d	-1.6	1.3	-0.4	0.3	-0.1	0.7	0.2	0.3	2.161
5	-Me, 6e	-2.5	1.2	1.8	-2.2	2.0	-0.4	-0.1	0.4	2.472
6	-SiMe ₃ , 6f	-2.96	1.42	0.27	-0.68	0.36	1.58	-0.01	—	1.990
7	S ⁺ (Me)(iPr), 6g	3	1	-2	1	-2	-2	-1	4	3.095 ^[a]
8	-C(O)Ph, 6h	-1.71	0.72	-0.38	0.53	-0.42	1.22	-0.04	—	2.681
9	-NH ₂ , 6i	-0.9	-0.3	0.9	-1.0	0.9	-0.3	-0.7	0.2	2.992
10	-OMe, 6j	0.7	-0.8	1.4	-1.5	2.8	-2.8	-0.2	0.4	3.543
11	-SO ₂ Me, 6k	0.2	-0.5	-0.2	1.0	-0.3	-0.2	-0.0	0.2	2.998
12	-C≡CPh, 6l	-0.2	-0.2	-0.9	0.8	0.9	-0.4	0.0	0.7	3.080
13	-P(iPr) ₂ , 6m	-2.8	1.1	0.3	-0.6	0.2	1.7	-0.1	0.2	2.249
14	-C(O)NH ₂ , 6n	-0.9	0.5	-0.5	0.6	0.3	-0.1	-0.1	0.3	2.731
15	-C(O)OMe, 6o	-0.6	-0.3	0.6	0.0	0.3	-0.1	-0.1	0.2	2.832

^[a] Approximate value taken from that established for -S⁺Me₂

Influence of the Electronegativity of a Substituent over the Value of Endocyclic Angles: the Case of Mono-Substituted and *para*-Disubstituted (η^6 -Arene)Cr(CO)₃ Complexes

A first approach involved the study of the angular distortion of mono-substituted (η^6 -arene)Cr(CO)₃ complexes. Retrieval of atomic coordinates of compounds **6a–o**^[15] from the CSDB allowed the measure of the endocyclic angles; the corresponding estimated standard deviation for the considered data were extracted from available published reports and averaged. In the cases of **6a**, **6f** and **6h**, exact values of $\sigma(\alpha)$ were not available to us. Among all the selected examples grouped in Table 2, only one complex, namely **6g**, presented a fairly high $\sigma(\alpha)$ value of 4 (entry 7, Table 2). However, this complex was considered, and the corresponding values of the endocyclic angle variations are provided.

Table 2 gives the values of Δ_i , deviations of the endocyclic angles from the ideal averaged value of 120.0 which was determined by the neutron-diffraction crystal structure of (η^6 -benzene)Cr(CO)₃.^[15b]

It can be noticed that almost all endocyclic angles deviate significantly from the ideal value. This is in contrast with observations made for uncoordinated aromatics. Indeed, it is generally observed that arene substituents cause significant distortions at the *ipso*, *ortho* and *meta* positions while *para* positions are mostly unaffected.^[9] Two points can be observed: first, two related *ortho* and *meta* positions display fairly different values of $\Delta_{2,6}$ and $\Delta_{3,5}$, and second, the value of Δ_4 is often different from zero (Table 2). The presence of the Cr(CO)₃ tripod on the one side of the arene induces a loss of symmetry and induces distortions of the arene ring that can be characterized by the sum of the endocyclic angular deviations $\Sigma\Delta_i$. The lower values of $\Sigma\Delta_i$ are obtained for the two aniline derivatives, **6c** (-0.7) and **6i** (-0.7), the acetophenone complex **6a**, and **6g**. A negative value of $\Sigma\Delta_i$ indicates an overall decrease in the value of endocyclic angles, a possible slight change of hybridization of the orbitals of aromatic carbons and thus an actual nonplanar nature of the aromatic ligand. For the compounds consid-

ered in this table, values of $\Sigma\Delta_i$ inferior in absolute value to $\sigma(\alpha)$ correspond to an almost planar arene ligand. Deviations of atomic position from the calculated least-square mean-aromatic planes confirm the significant distortions for **6c**, **6i**, **6a**, **6g** and corroborate the information suggested by values of $\Sigma\Delta_i$. A plot of the *ipso* endocyclic distortion versus the electronegativity of the group as defined and calculated by Inamoto,^[16] confirms that mono-substituted arene complexes follow a trend similar to that of uncoordinated arenes. Figure 4 presents a scattered distribution of data points around a mean diagonal line.

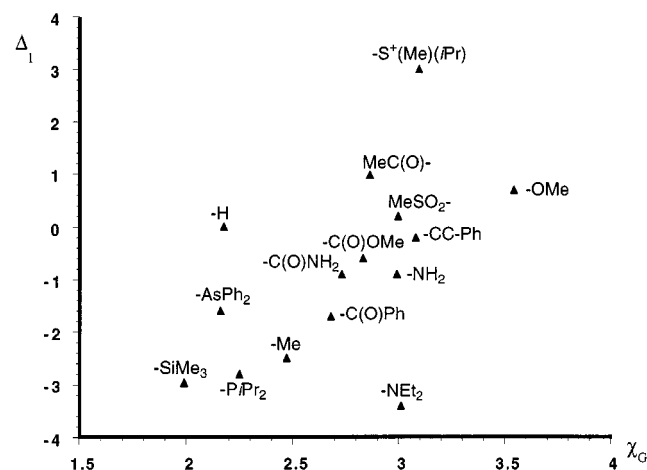
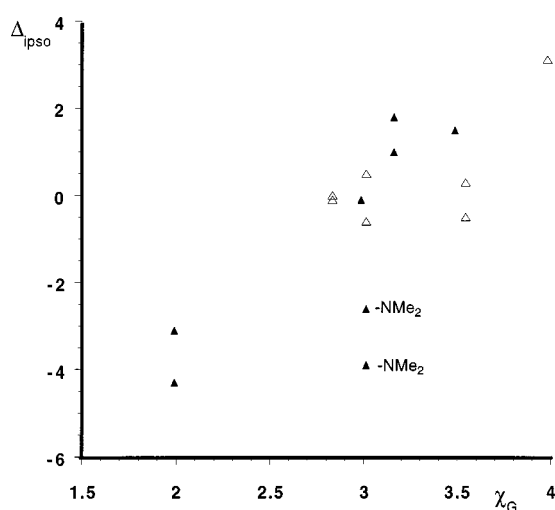


Figure 4. Graph of Δ_{ipso} (deg) versus χ_G for mono-substituted arene complexes

Few points are positioned out of the main statistical cloud. These data points correspond to arene complexes substituted by -NEt₂ (**6c**), -S⁺(Me)(iPr) (**6g**), -C(O)Me (**6a**). Strikingly, the data point corresponding to the benzene complex is found outside the statistical ascending cloud that groups together data from compounds **6f**, **6m**, **6d**, **6h**, **6n**, **6o**, **6i**, **6l**, **6k** and **6j**. This could be in part due to an underestimation of the value of χ_G for -H in aromatic compounds. It is known that the electronegativity of a given group may take significantly different values depending on

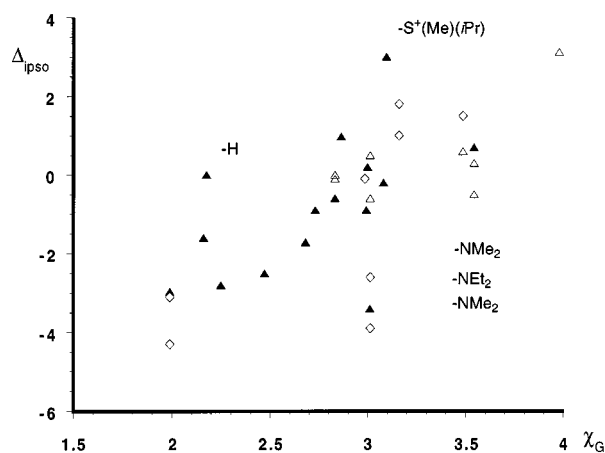
Table 3. Endocyclic *ipso*-carbon angular deviations at C1 (deg). Raw and corrected values listed with electronegativity χ_G of the group connected at C1

entry	groups, compound	Δ_1 (deg)	$\Delta_{1\text{corr}}$ (deg)	Δ_4 (deg)	$\sigma(a)$	χ_{G1}
1	1-H, 4-CH(OMe) ₂ , 6p	-0.24		-1.93		
2	1-H, 4-CH(OEt) ₂ , 6q	-0.37		-1.11		
3	1-NMe ₂ , 4-CH(OMe) ₂ , 7a	-4.0	-3.9		0.4	3.012
4	1-NMe ₂ , 4-CH(OEt) ₂ , 7b	-3.0	-2.6		0.5	3.012
5	1-Cl, 4-CH(OMe) ₂ , 7c	1.5	1.8		0.9	3.16
6	1-Cl, 4-CH(OEt) ₂ , 7d	0.7	1.0		0.7	3.16
7	1-SiMe ₃ , 4-CH(OMe) ₂ , 7e	-3.4	-3.1		0.4	1.990
8	1-SiMe ₃ , 4-CH(OEt) ₂ , 7f	-4.7	-4.3		0.4	1.990
9	1-CF ₃ , 4-CH(OMe) ₂ , 7g	-0.4	-0.1		0.7	2.985
10	1-CF ₃ , 4-CH(OEt) ₂ , 7h	-0.5	-0.1		0.2	2.985
11	1,4-F ₂ -F, 7i	3.12		3.12	0.2	3.98
12	1-OCF ₃ , 4-NH ₂ , 7j	0.6	1.5		0.2	3.486
13	1,4-OMe, -OMe, 7k	-0.5		0.3	0.7	3.543
14	1,4-NMe ₂ , -NMe ₂ , 7l	0.5		-0.6	0.5	3.012
15	1,4-CO ₂ Me, -CO ₂ Me, 7m	0.0		-0.1	0.3	2.832

Figure 5. Graph of Δ_{ipso} (deg) versus χ_G for *para*-disubstituted arene complexes: (▲) compounds **7a–h** and **7j**; (△) compounds **7i** and **7k–m**

the nature of the organic or inorganic radical connected to it.^[17] Therefore the plot displayed in Figure 4 must be considered as an informative qualitative picture.

We have applied a similar treatment to selected examples of hetero- and homo- *para*-disubstituted complexes bearing various types of substituents. For compounds **7a–h**^[18] the endocyclic angular distortion at aromatic carbon 1 bearing the considered substituent located *para* to the acetal group –CH(OR)₂, was corrected for the distortions caused by the latter group. The correction terms applied to Δ_1 of compounds **7a–h** in Table 3, were extracted from the value of the *para* endocyclic angular deviations Δ_4 in the molecular structures of mono-substituted complexes **6p–q**. This consequently allowed the determination of approximated values of Δ_{ipso} for the following substituents: –NMe₂, Cl, SiMe₃, CF₃. A similar treatment was applied to values extracted from the molecular structure of compound **7j**^[19] in order to obtain a corrected value of Δ_{ipso} for –OCF₃; this was carried out by applying a correction term which corresponded to the value of Δ_4 of the aniline complex **6i**. For

Figure 6. Graph of Δ_{ipso} (deg) versus χ_G for mono-substituted and *para*-disubstituted arene complexes: (▲) compounds **6a–o**; (△) homo-disubstituted compounds **7i**, **7k–m**; (◇) hetero-disubstituted compounds **7a–h**, **7j**

the *para*-homo-disubstituted complexes **7i**,^[20] **7k–m**, no corrections were applied to the values of Δ_1 and Δ_4 .

A plot of these corrected and uncorrected values of Δ_{ipso} versus χ_G is displayed in Figure 5. A combination of the data of Table 2 and 3 allowed us to establish a new graph (Figure 6) in which it can clearly be seen that the value of the *ipso* carbon endocyclic angular deviation correlates with the Inamoto group and Pauling element^[21] electronegativity χ_G , unless resonance interactions perturb such a phenomenon as in complexes bearing –NR₂ (R = Me, Et), and the isolobal –S⁺RR' group. Electronegativities of substituents play a significant part in the overall distortion of the aromatic ring of (η^6 -arene)Cr(CO)₃ complexes.

Correlation of Metal-to-Ring Distances with Hammett Constants in Monosubstituted (η^6 -arene)Cr(CO)₃ Complexes: Nonlinear and Linear Correlations of the C_{ipso} –Cr and the Metal-to-Ring Mean-Plane Distances with σ_p

Metal to aromatic carbon distances have been often reported to be influenced by the “electron richness” of the

Table 4. List of values of d_{ipso} , d_0 (in Å) of mono-substituted arene complexes (η^6 -G-C₆H₅)Cr(CO)₃ and Hammett substituent constants σ_p , σ_p^+ and σ_p^-

entry	–G, compound	d_{ipso} (Å)	$\sigma(d_{ipso})$ (Å)	d_0 (Å)	σ_p	σ_p^+	σ_p^-
1	–C(O)Me, 6a	2.157	0.008	1.700	0.50	–	0.84
2	–H, 6b	2.230	0.003	1.725	0.00	–	–
3	–NEt ₂ , 6c	2.369	0.002	1.748	–0.72	–2.07	–0.43
4	–AsPh ₂ , 6d	2.219	0.003	1.708	0.09	–	0.29
5	–Me, 6e	2.236	0.004	1.725	–0.17	–0.31	–0.17
6	–SiMe ₃ , 6f	2.239	0.004	1.722	–0.07	0.02	–
7	–S ⁺ (Me)(iPr), 6g	2.140	0.05	1.671	0.90 ^[a]	–	0.83 ^[a]
8	–C(O)Ph, 6h	2.193	–	1.694	0.43	0.51	0.83
9	–NH ₂ , 6i	2.349	0.003	1.745	–0.66	–1.30	–0.15
10	–OMe, 6j	2.264	0.005	1.740	–0.27	–0.78	–0.26
11	–SO ₂ Me, 6k	2.172	0.002	1.682	0.72	–	1.13
12	–CCPh, 6l	2.206	0.006	1.695	0.16	–0.03	0.30
13	–PiPr ₂ , 6m	2.231	0.002	1.710	0.06	–	–
14	–C(O)NH ₂ , 6n	2.210	0.002	1.699	0.36	–	0.61
15	–C(O)OMe, 6o	2.214	0.002	1.714	0.45	0.49	0.75

^[a] Approximate value taken from –S⁺Me₂.

aromatic ring and many authors pointed out indirectly that this parameter was a sensitive probe for assessing the magnitude of electron density transfer within (η^6 -arene)Cr(CO)₃ complexes.^[19] We decided to verify whether variations of d_{ipso} and d_0 could be linked to quantified effects such as inductive or resonance effects of substituents connected to the ring. Table 4 lists the values of d_{ipso} and d_0 obtained from structural information. All standard deviations $\sigma(d_{ipso})$ were obtained from the corresponding published reports except for **6h** (entry 8, Table 4); in the case of compound **6a** (entry 1, Table 4), a geometric $\sigma(d)$ value was calculated from the standard deviations of the atomic coordinates extracted from the published report. It must be noted that d_0 was determined by considering the mean-plane, including all six arene carbons, even in strongly distorted rings: in doing so we established a reliable way of “idealizing” the distortion of the arene as even in strongly distorted molecules, the p-orbital at C_{*ipso*} is supposedly still engaged in aromaticity^[22] and in a bonding interaction with the Cr atom. In many previous reports Cr-to-ring distances were calculated without taking into account the *ipso* carbon bearing the “perturbing” substituent, thus leading to a systematic underestimation of the value of d_0 .

A plot of d_{ipso} versus the Hammett constant σ_p for various substituents^[23] is given in Figure 7. The constant σ_p is defined for reactions taking place at a reactive site located *para* to a substituent, a position greatly favored by both inductive and resonance effects. For a given substituent of an aromatic compound, the σ_p constant is approximately the sum of the contributions of the inductive/field parameter, F , and the resonance parameter, R .^[24] As can be noticed from Figure 7, there is a clear nonlinear correlation between the two parameters d_{ipso} and σ_p . A much better result is obtained by plotting d_{ipso} versus σ_p^+ . The Hammett constant σ_p^+ has been devised for substituents conjugated with a reaction center which could effectively delocalize a positive charge.^[25] As a result, values of σ_p^+ for π -electron donor substituents are considerably enhanced relative to the corresponding σ_p . The former σ_p^+ Hammett constant seems more appropriate in our study as the

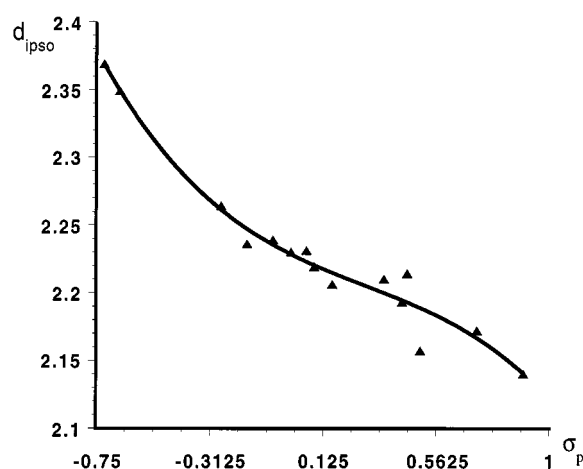


Figure 7. Plot of d_{ipso} (Å) versus σ_p for mono-substituted arene complexes

Cr(CO)₃ moiety decreases π -electron density on the aromatic ring and acts in a similar manner to an π -electron-withdrawing arene substituent inducing the creation of a positive charge in the Cr-arene segment; Kinomura and co-workers^[26] have evaluated the partial charges in (η^6 -benzene)Cr(CO)₃ to be –0.12e at benzene, +0.54e at the chromium atom, +0.15e at carbonyl carbons and –0.29e at carbonyl oxygen. Figure 8 displays a linear correlation between d_{ipso} and σ_p^+ which can be formulated by the following least-squares Equation:

$$d_{ipso} = 2.23 (\pm 0.01) - 0.07 (\pm 0.01) \times \sigma_p^+ \quad (n = 6, R = 0.955, \chi^2 = 0.002).$$

The value of the intercept corresponds exactly to the value of d_{ipso} for the reference compound (η^6 -benzene)Cr(CO)₃, **6b**. Figure 9 displays a plot of d_{ipso} versus σ_p^- which affords, according to expectations, a nonlinear relationship between the two parameters.

A plot of d_0 versus σ_p gives a distribution of points that strongly suggests a linear relationship between the two

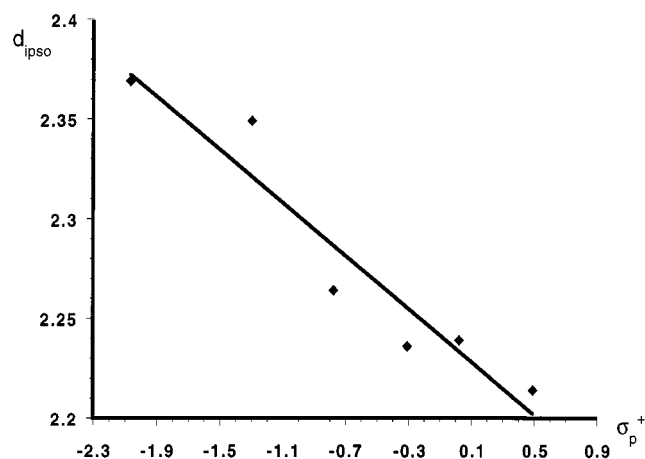


Figure 8. Plot of d_{ipso} (Å) versus σ_p^+ for mono-substituted arene complexes

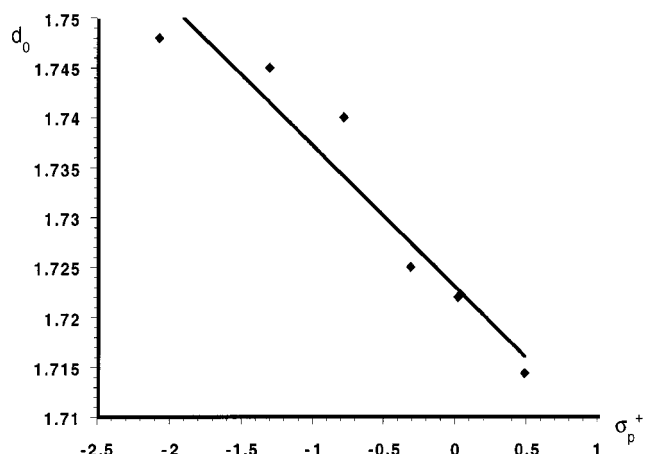


Figure 11. Plot of d_0 (Å) versus σ_p^+ for mono-substituted arene complexes

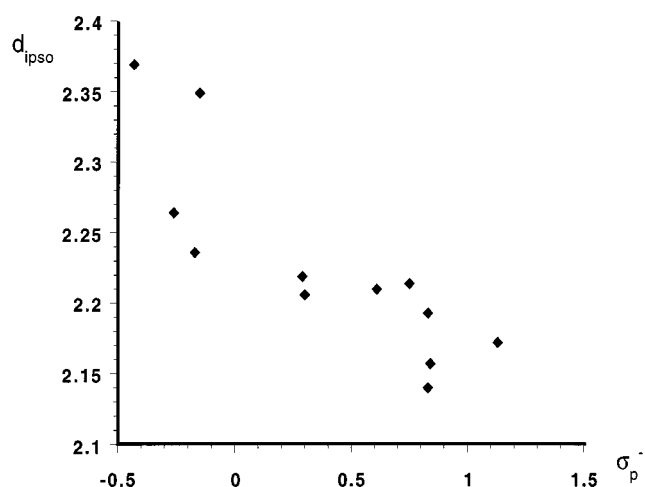


Figure 9. Plot of d_{ipso} (Å) versus σ_p^- for mono-substituted arene complexes

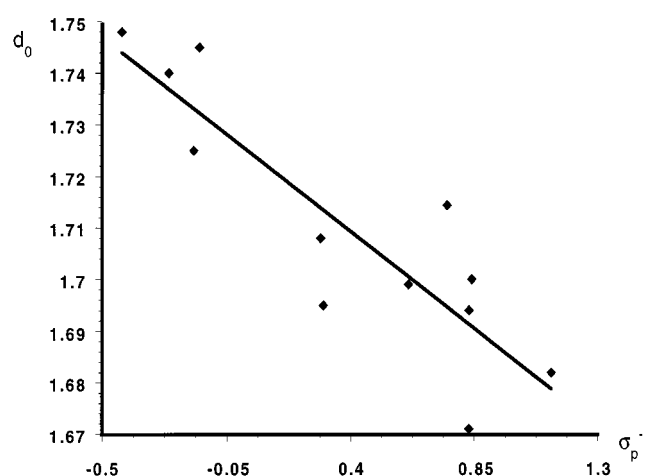


Figure 12. Plot of d_0 (Å) versus σ_p^- for mono-substituted arene complexes

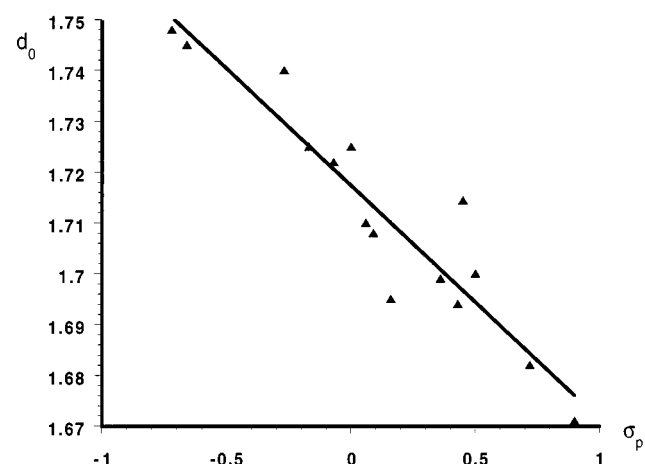


Figure 10. Plot of d_0 (Å) versus σ_p for mono-substituted arene complexes

parameters (Figure 10). A curve fitting carried out by the least-squares method affords the following linear relationship between d_0 and σ_p for the mono-substituted arene complexes in question:

$$d_0 = 1.717(\pm 0.002) - 0.045(\pm 0.004) \times \sigma_p, \quad (n = 15, \chi^2 = 0.0008, R = 0.939).$$

Here the intercept is significantly lower than the value of 1.725 Å measured for the reference compound **6b**. Interestingly, plots of d_0 versus σ_p^+ (Figure 11) and σ_p^- (Figure 12) give more convincing values for the intercept, although the value of the correlation coefficient R for the expression involving σ_p^- is not optimal. The least-squares fitting carried out from the latter plots affords the following Equations:

$$d_0 = 1.723(\pm 0.002) - 0.014(\pm 0.002) \times \sigma_p^+ \quad (n = 6, \chi^2 = 7 \times 10^{-5}, R = 0.959)$$

and

$$d_0 = 1.726(\pm 0.004) - 0.041(\pm 0.007) \times \sigma_p^- \quad (n = 12, \chi^2 = 0.001, R = 0.880).$$

Application of this relationship to the determination of σ_p of the two acetal groups $-\text{CH}(\text{OMe})_2$ ($d_0 = 1.717$ Å in **6p**) and $-\text{CH}(\text{OEt})_2$ ($d_0 = 1.709$ Å in **6q**) affords values of 0.00 and 0.17 respectively which compare satisfactorily with those established for $-\text{CH}(\text{OMe})_2$ (σ_p value calculated

Table 5. List of values of d_{ipso} (Å) for hetero- and homo-disubstituted arene complexes and the corresponding Hammett substituent constants σ_p , σ_p^+ and σ_p^-

entry	compound	-G	$d_{ipso}(\sigma(d_{ipso}))$	σ_p	σ_p^+	σ_p^-
1	7a	1-NMe ₂	2.382(4)	-0.83	-1.70	-0.12
		4-CH(OMe) ₂	2.230(4)	0 ^[a]		
2	7b	1-NMe ₂	2.377(5)	-0.83	-1.70	-0.12
		4-CH(OEt) ₂	2.218(5)	0.17 ^[a]		
3	7c	1-Cl	2.217(7)	0.23	0.11	0.19
		4-CH(OMe) ₂	2.213(7)	0 ^[a]		
4	7d	1-Cl	2.204(4)	0.23	0.11	0.19
		4-CH(OEt) ₂	2.203(4)	0.17 ^[a]		
5	7e	1-SiMe ₃	2.230(4)	-0.07	0.02	
		4-CH(OMe) ₂	2.227(4)	0 ^[a]		
6	7f	1-SiMe ₃	2.240(4)	-0.07	0.02	
		4-CH(OEt) ₂	2.233(3)	0.17 ^[a]		
7	7g	1-CF ₃	2.195(6)	0.54	0.61	0.65
		4-CH(OMe) ₂	2.217(6)	0 ^[a]		
8	7h	1-CF ₃	2.194(2)	0.54	0.61	0.65
		4-CH(OEt) ₂	2.207(2)	0.17 ^[a]		
9	7i	1-F	2.215(4)	0.06	-0.07	-0.03
		4-F	2.215(4)	0.06	-0.07	-0.03
10	7j	1-OCF ₃	2.199(2)	0.35		0.27
		4-NH ₂	2.353(2)	-0.66	-1.30	-0.15
11	7k	1-OCH ₃	2.262(6)	-0.27	-0.78	-0.26
		4-OCH ₃	2.292(6)	-0.27	-0.78	-0.26
12	7l	1-NMe ₂	2.322(5)	-0.83	-1.70	-0.12
		4-NMe ₂	2.207(5)	-0.83	-1.70	-0.12
13	7m	1-CO ₂ Me	2.199(3)	0.45	0.49	0.75
		4-CO ₂ Me	2.189(3)	0.45	0.49	0.75
14	3	1-NMe ₂	2.410(10)	-0.83	-1.70	-0.12
		3-CF ₃	2.170(9)	0.54	0.61	0.65
15	4	1-NMe ₂	2.348(7)	-0.83	-1.70	-0.12
		3-SiMe ₃	2.247(6)	-0.07	0.02	
16	7n	1- <i>i</i> Bu	2.251(6)	-0.20	-0.26	-0.13
		4-C(O)OH	2.170(6)	0.45	0.42	0.77
17	8a	1-OH	2.33(3)	-0.37	-0.92	-0.37
		2-C(O)Me	2.15(2)	0.50		0.84
18	8b	1-OMe	2.28(3)	-0.27	-0.78	-0.26
		2-C(O)Me	2.24(2)	0.50		0.84
19	8c	1-NH ₂	2.37(1)	-0.66	-1.30	-0.15
		2-Me	2.26(1)	-0.17	-0.31	-0.17
20	5	1-NMe ₂	2.383(3)	-0.83	-1.70	-0.12
		2-C(O)OMe	2.232(3)	0.45	0.49	0.75

[a] Calculated value.

from ^{19}F NMR = 0.03) and other analogous groups such as $-\text{CH}_2\text{OMe}$ (0.01), and $-\text{C(OMe)}_3$ (-0.04). Accordingly, σ_p^+ and σ_p^- values for the two aforementioned acetal groups are estimated from the corresponding values of d_0 in **6p–q** as being equal to 0.43 and 0.22 for $-\text{CH(OMe)}_2$ and 1.0 and 0.41 for $-\text{CH(OEt)}_2$, respectively.

Disubstituted Arene Complexes

Values of d_{ipso} for a variety of *para*, *meta* and *ortho* disubstituted arene complexes are grouped in Table 5; *para*-disubstituted arene complexes are compounds **7a–m** and **7n**,^[27] *meta*-disubstituted arene complexes are compounds **3–4**, *ortho*-disubstituted arene complexes are compounds **8a–b**,^[28] and **8c**,^[29] and **5**. A plot of d_{ipso} versus σ_p is given in Figure 13 and shows a nonlinear distribution of the data points. The largest scattering of the data points in Figure 13 is observed for the $-\text{NMe}_2$ groups in the disymmetric *para*-homodisubstituted complex **7l**, for $-\text{C(O)Me}$ in **8a** and **8b** and for $-\text{C(O)OMe}$ in **5**. In the three latter cases which correspond to *ortho*-disubstituted arene complexes the deviation, may be attributed to the predominant electronic ef-

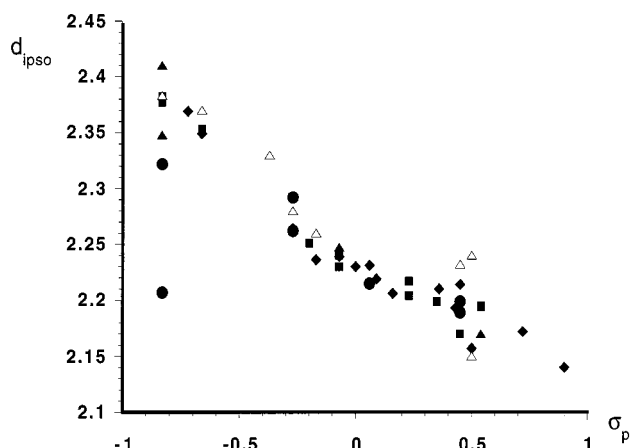


Figure 13. Plot of d_{ipso} (Å) versus σ_p for mono- and di-substituted arene complexes: (▲) compounds **3** and **4**; (■) compounds **7a–h** and **7n**; (◆) compounds **6a–o**; (●) compounds **7i** and **7k–m**; (△) compounds **8a–b**, **8c** and **5**

fects imposed by $-\text{OH}$, $-\text{OMe}$ and NMe_2 groups over the shifting of the Cr(CO)_3 moiety; such predominant electronic effects may induce exaggerated values of d_{ipso} for the vicinal *ortho*-position depending on the privileged direction of the shift of the chromium atom in the tripod.

Combined values of d_{ipso} for mono- and di-substituted arene complexes (except those from **8a–c**, **5** and **7l**) are plotted versus σ_p in Figure 13. The shape of the plot assesses the dependency of d_{ipso} on both the inductive and resonance effects of a given aromatic substituent. It shows a relative independence towards the position and the nature of a second substituent of the arene ring (as long as it is not located at the *ortho* position).

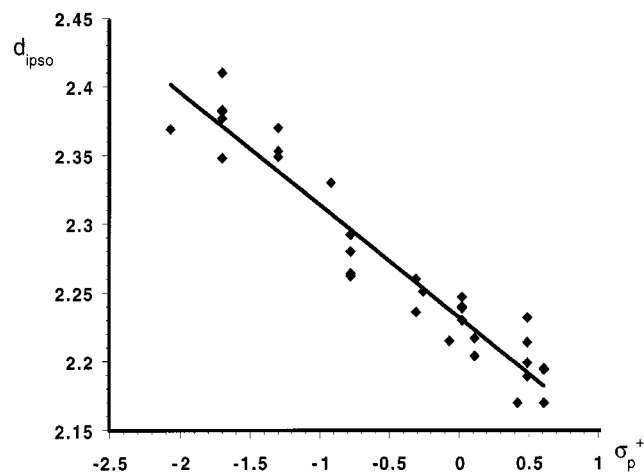


Figure 14. Plot of d_{ipso} (Å) versus σ_p^+ for mono- and di-substituted arene complexes having a defined value of the considered Hammett constant.

A plot of d_{ipso} versus σ_p^+ (Figure 14) that includes the data provided by the structures of *meta*-disubstituted arene complexes and excludes those of **8a–c**, **5** and **7l**, indicates now a clear linear relationship between the two parameters which is illustrated by the following linear Equation:

$$d_{ipso} = 2.232(\pm 0.004) - 0.082(\pm 0.005) \times \sigma_p^+ \quad (n = 33, \chi^2 = 0.013, R = 0.959).$$

Table 6. List of values of d_0 (Å) for *para*-disubstituted arene complexes

entry	compound	substituents	d_0 (Å)
1	7a	1-NMe ₂ , 4-CH(OMe) ₂	1.751
2	7b	1-NMe ₂ , 4-CH(OEt) ₂	1.750
3	7c	1-Cl, 4-CH(OMe) ₂	1.709
4	7d	1-Cl, 4-CH(OEt) ₂	1.703
5	7e	1-SiMe ₃ , 4-CH(OMe) ₂	1.716
6	7f	1-SiMe ₃ , 4-CH(OEt) ₂	1.714
7	7g	1-CF ₃ , 4-CH(OMe) ₂	1.702
8	7h	1-CF ₃ , 4-CH(OEt) ₂	1.702
9	7i	1-F, 4-F	1.718
10	7j	1-OCF ₃ , 4-NH ₂	1.743
11	7k	1-OCH ₃ , 4-OCH ₃	1.759
12	7l	1-NMe ₂ , 4-NMe ₂	1.756
13	7m	1-CO ₂ Me, 4-CO ₂ Me	1.698

Here again, the value of the intercept fits the value of d_{ipso} for (η^6 -benzene)Cr(CO)₃, **6b**.^[15b] Values of σ_p^+ for the acetal groups –CH(OMe)₂ and –CH(OEt)₂ have been recalculated from the corresponding averaged values of d_{ipso} (e.g. $\langle d_{ipso} \rangle$) extracted from the structures of **6p–q** and **7a–h** and by applying the latter Equation. The following values were obtained and differ from those obtained from the aforementioned Equations based on the parameters d_0 of mono-substituted arene complexes: for –CH(OMe)₂ ($\langle d_{ipso} \rangle = 2.223$ Å), $\sigma_p^+ = 0.11$; for –CH(OEt)₂ ($\langle d_{ipso} \rangle = 2.217$ Å), $\sigma_p^+ = 0.18$. As for such substituents no peculiar resonance effect may be expected. The two values of σ_p^+ determined here are in our opinion more acceptable than those obtained from the previous correlation, as they are fairly close to the values reported for structurally similar groups such as –CH₂OCH₃ ($\sigma_p^+ = -0.05$) and –CH₂OH ($\sigma_p^+ = -0.04$).^[23]

Again, we find that d_{ipso} does not correlate with the σ_p^- substituent constants (graph not shown).

Values of d_0 for *para*-disubstituted complexes have been calculated in several examples and are presented in Table 6. They display a nonlinear dependence of d_0 versus the sum of the σ_p values for each substituent connected to the arene ligand (plot not shown here). We were not successful in establishing a simple relationship that would link d_0 either to the respective substituent electronic effects or to the molecular dipolar moment of the molecule which is presumably oriented from the arene ring to the chromium atom along the d_0 axis.^[30] However, it may be noted that the value of d_0 for a given *meta*- or *para*-disubstituted arene complex is certainly significantly influenced by the values of the d_{ipso} parameter of a given substituent.

On the Prediction of the Distortions in (η^6 -Arene)tricarbonylchromium Complexes

Hence, the d_{ipso} and d_0 parameters appear to be two intrinsic constraints imposed by the electronic properties of a given substituent over the geometric position of the Cr(CO)₃. Therefore, the main structural features of arene complexes can be predicted for mono- as well as *meta* and *para* di-substituted arene complexes regardless of the con-

formation of the Cr(CO)₃ tripod. Provided that σ_p^+ constants are established for the most common groups, it should now be possible to predict the approximate position of the Cr atom relative to the relevant C_{ipso} positions. A combination of effects related to the electronegativity, the resonance and the inductive properties of a given substituent governs the overall geometry of the arene ligand. It appears that a strong resonance effect such as that produced by amino groups emphasizes, in a rather predictable way on the basis of Hammett's σ_p^+ constants, the electronic repulsion between the Cr-centered moiety and the *ipso* position. A strong substituent resonance effect concomitantly causes a decrease of the *ipso* endocyclic angle at C_{ipso} and an increase of the related d_{ipso} value thus conceding a significant folding of the arene ligand.

Conclusion

In this article we have established that the distortions of the arene ligand in (η^6 -arene)Cr(CO)₃ complexes are influenced by the electronegativity, the inductive and the resonance effects of arene substituents. We have shown that endocyclic angular deviations at a carbon substituted by a given substituent was generally directed by the electronegativity of the latter in the absence of perturbing resonance effects. It was shown that mesomeric effects could partially obliterate electronegativity based effects. We have also demonstrated that the chromium-to-*ipso*-carbon distance is a specific constraint imposed to the molecular spacial arrangement by the electronic properties of an arene substituent. It was established that d_{ipso} correlates linearly with σ_p^+ Hammett constants, providing us with the confirmation of a relevant participation of electrons of the σ -framework in the metal-arene ring bonding interaction and with an understanding of the role of resonance effects in the overall structural distortions. Further investigations on the possible deduction of the value of Hammett constants for uncommon organic and organometallic substituents from the structural parameters of (η^6 -arene)tricarbonyl chromium complexes are currently in progress.

Experimental Section

General Remarks: All reactions were carried out under a dry nitrogen atmosphere. The complexes were, in general, stable in the solid state, in air for long periods of time. Consequently, all experiments involving arenetricarbonylchromium complexes were protected from exposure to light and oxygen. Tetrahydrofuran (THF) and di-*n*-butyl ether (DBE) were dried over sodium benzoketyl under dry nitrogen and distilled just before use. Products were separated by flash chromatography on a silica gel column (15 or 60 μ m) under a dry positive nitrogen pressure. Diethyl ether (Et₂O) and petroleum ether were used as solvents for elution. – ¹H and ¹³C NMR spectra were acquired on a Bruker AC 200 (resonance frequencies: 200 MHz for ¹H and 50 MHz for ¹³C) spectrometer and chemical shifts were reported in parts per million downfield of Me₄Si. ¹H NMR spectra were referenced against the residual ¹H impurity of the deuterated solvent and ¹³C NMR spectra were referenced

against the ^{13}C resonance of the solvent. – Infrared spectra (reported in cm^{-1}) were performed on Perkin–Elmer 1420 and Bruker FT spectrometers. – Elemental analyses (reported in % mass) were performed by “Le Service de Microanalyses de l’Université P. et M. Curie”. The crystallographic information files (CIF) provided by the CSDB were analyzed with ORTEP-3^[31] version 1.03 and ORTEX-6b^[32] software. The CSDB acronyms for some of the structures of monosubstituted arene complexes studied in this paper are the following: **6a**, ACTPCR; **6b**, BZCRCO12; **6c**, ANLCRA10; **6d**, ASPHCR; **6e**, CCRTOL; **6f**, CMSICR; **6g**, CRSLFN; **6h**, DEDHAV; **6i**, KOZROG; **6j**, KOZRUM; **6k**, LEPNEZ; **6l**, RAYJAC; **6m**, RIHPED; **6n**, POLTUF.

Preparation of (η^6 -*N,N*-Dimethyl-3-trimethylsilylaniline)tricarbonylchromium, Complex 3:^[4] A solution of *n*BuLi (1.6 M, 3.0 mL, 4.8 mmol) in hexane was added dropwise to a solution of 2,2,6,6-tetramethylpiperidine (678 mg, 0.81 mL, 4.8 mmol) in THF (10 mL) at -78°C . The resulting medium was stirred for 10 min and a solution of **1** (1.0 g, 4 mmol) in THF (10 mL) was added. The resulting mixture was stirred for an additional 30 min at -78°C and Me_3SiCl was added (1.3 g, 1.53 mL, 12.0 mmol) dropwise. The reaction medium was slowly warmed to room temperature and extracted with Et_2O . The organic phase was washed with water and brine, dried over MgSO_4 , filtered through Celite and the solvents removed by vacuum distillation. The yellow residue was purified by flash chromatography over silica gel. The starting substrate was first eluted (petroleum ether 100%), followed by complex **2** (Et_2O /petroleum ether = 10:90) and complex **3** (Et_2O /petroleum ether = 20:80). Recrystallization in pentane afforded complexes **2** (200 mg, 0.61 mmol, 15% yield) and **3** (739 mg, 2.25 mmol, 57% yield).

Preparation of (η^6 -*N,N*-Dimethyl-3-trifluoromethylaniline)tricarbonylchromium, Complex 4: *N,N*-Dimethyl-3-trifluoromethylaniline (9.45 g, 50.0 mmol), $\text{Cr}(\text{CO})_6$ (11 g, 50.0 mmol), THF (15 mL), *n*Bu₂O (150 mL), 6 days. Yield of **4**: 61% (10.0 g). – M.p. 116°C . – MS (IE); *m/z*: 325 (M^+). – $\text{C}_{12}\text{H}_{10}\text{F}_3\text{NCrO}_3$ (325.2): calcd. C 44.32, H 3.10, N 4.31; found C 44.26, H 3.10, N 4.19. – IR (nujol):

$\tilde{\nu} = 1950, 1865 (\text{C}=\text{O}) \text{ cm}^{-1}$. – ^1H NMR (C_6D_6): $\delta = 4.64$ (t, $^3J = 7 \text{ Hz}$, 1 H, H-5), 4.43 (d, $^3J = 7 \text{ Hz}$, 1 H, H-4), 4.41 (d, $^4J = 1.5 \text{ Hz}$, 1 H, H-2), 3.75 (dd, $^3J = 7 \text{ Hz}$, $^4J = 1.5 \text{ Hz}$, 1 H, H-6), 1.87 (s, 6 H, NMe₂). – ^{13}C NMR (CDCl_3): $\delta = 39.7$ ($(\text{CH}_3)_2\text{-N}$), 68.8–73.8–79.4–94.4 (C-2, C-4, C-5, C-6), 101.5 (q, $^2J = 30 \text{ Hz}$, C-3), 130.0 (q, $^1J = 120 \text{ Hz}$, CF_3), 133.7 (C-1), 232.9 (CO).

(η^6 -*N,N*-Dimethyl-2-methoxycarbonylaniline)tricarbonylchromium, Complex 5: $\text{C}_{13}\text{H}_{13}\text{O}_5\text{NCr}$ (315.2): calcd: C 49.62, H 4.13, N 4.44; found C 49.82, H 4.23, N 4.48. – IR (CCl_4): $\tilde{\nu} = 1997, 1938 (\text{C}=\text{O})$, 1735 $[\text{C}(\text{O})\text{OMe}] \text{ cm}^{-1}$. – ^1H NMR (CDCl_3): $\delta = 2.83$ (s, 6 H, NMe₂), 3.87 (s, 3 H, OCH₃), 4.84 (t, $J = 6 \text{ Hz}$, 1 H, H-4), 4.97 (d, $J = 6 \text{ Hz}$, 1 H, H-6), 5.67 (t, $J = 6 \text{ Hz}$, 1 H, H-5), 6.04 (d, $J = 6 \text{ Hz}$, 1 H, H-3). – ^{13}C NMR (CDCl_3): $\delta = 42.7$ (N(CH₃)₂), 52.9 (OCH₃), 76.5, 82.6, 96.6, 98.4 (C_{3–6}), 82.4 (C₂), 136.7 (C₁), 165.5 (C(O)OMe), 238.8 (Cr–CO).

Structural Determination of Complexes 3, 4, 5. Intensity data were collected at room temperature on an Enraf–Nonius CAD4 diffractometer using Mo-K_α radiation. Accurate cell dimensions and orientation matrices were obtained from least-square refinements of the setting angles of 25 well-defined reflections. No decay in the intensities of two standard reflections was observed during the course of the data collections. Complete crystal data, collection parameters and other significant details are listed in Table 7.

The usual corrections for Lorentz and polarization effects were applied. Computations were performed by using CRYSTALS.^[33] Scattering factors and corrections for anomalous dispersion were taken from the International Table for X-ray Crystallography.^[34] The structures were resolved by direct methods (SHELXS 86^[35]) and refined by least squares with anisotropic thermal parameters for all nonhydrogen atoms. For compound **4**, hydrogen atoms were located on a Fourier difference map and introduced as fixed contributors in the last refinements with an overall refinable isotropic thermal parameter. The structure was refined to $R = 0.031$ with the use of 1813 reflections for 22 least-squares parameters. For compound **3**, hydrogen atoms were introduced as fixed contributors in theoretical posi-

Table 7. Acquisition and data refinement parameters for compounds **3–5**

Compound	3	4	5
empirical formula	$\text{C}_{14}\text{H}_{19}\text{CrNO}_3\text{Si}$	$\text{C}_{12}\text{H}_{10}\text{CrF}_3\text{NO}_3$	$\text{C}_{13}\text{H}_{13}\text{CrNO}_5$
formula mass ($\text{g}\cdot\text{mol}^{-1}$)	329.4	325.2	315.2
crystal system	orthorhombic	monoclinic	monoclinic
space group	$P2_12_12_1$	$P2_1/c$	$P2_1/n$
<i>a</i> (Å)	7.640(4)	11.542(3)	11.720(2)
<i>b</i> (Å)	11.901(3)	7.097(3)	8.791(1)
<i>c</i> (Å)	17.736(3)	15.920(4)	14.271(2)
β (deg)		99.23(2)	110.36(1)
<i>V</i> (Å ³)	1612(1)	1287(4)	1378(6)
<i>Z</i>	4	4	4
<i>F</i> (000)	688	656	648
<i>d</i> _{calcd.} ($\text{g}\cdot\text{cm}^{-3}$)	1.36	1.68	1.52
μ (Mo-K_α) (cm^{-1})	7.69	9.07	8.25
crystal size (mm)	$0.14 \times 0.14 \times 0.80$	$0.06 \times 0.16 \times 0.70$	$0.22 \times 0.43 \times 0.50$
diffractometer	CAD4	CAD4	CAD4
monochromator	graphite	graphite	graphite
radiation	Mo-K_α (0.71070 Å)	Mo-K_α (0.71070 Å)	Mo-K_α (0.71070 Å)
<i>T</i> (°C)	20	20	20
scan type	$\omega/2\theta$	$\omega/2\theta$	$\omega/2\theta$
2θ range (deg)	2–50	3–40	3–50
no of reflns collected	1637	1194	2414
no of reflns observed	1107 ($I > 3\sigma(I)$)	908 ($I > 3\sigma(I)$)	1813 ($I > 3\sigma(I)$)
<i>R</i>	0.0361	0.0491	0.031
<i>R</i> _w [a]	0.0381	0.0520	0.032
absorption correction	min. 0.81, max. 1.09	min. 0.76, max. 1.38	min. 0.87, max. 1.10
no of parameters	183	182	222

[a] $R_w = [\sum_i W_i (F_o - F_c)^2 / \sum_i W_i F_o^2]^{1/2}$

tions and their coordinates were recalculated after each refinement. The structure was refined to $R = 0.036$ with the use of 1107 reflections for 183 least square parameters. Crystallographic data (excluding structure factors) for the structures reported in this paper have been deposited with the Cambridge Crystallographic Data Centre as supplementary publications no. CCDC-135688 (4), -135689 (3), -135690 (5). Copies of the data can be obtained free of charge on application to The Director, CCDC, 12 Union Road, Cambridge CB2 1EZ, UK [Fax: (internat.) + (1223) 336-033; E-mail: deposit@ccdc.cam.ac.uk].

Acknowledgments

We thank the CNRS for supporting this work.

- [1] [1a] M. F. Semmelhack, *Ann. N. Y. Acad. Sci.* **1977**, 295, 36–51. — [1b] G. Jaouen, *Ann. N. Y. Acad. Sci.* **1977**, 295, 59–78. — [1c] S. G. Davies, *Organotransition Metal Chemistry, Applications to Organic Syntheses*, Pergamon Press, Oxford, U.K., **1982**, p 166. — [1d] W. E. Watts, *Comprehensive Organometallic Chemistry* Pergamon Press, Oxford, U.K., **1982**, p 1013. — [1e] A. Solladié-Cavallo, *Polyhedron* **1985**, 4, 901–927. — [1f] V. N. Kalinin, *Russ. Chem. Rev.* **1987**, 56, 682–700. — [1g] M. F. Semmelhack, *Comprehensive Organic Synthesis* (Ed: B. M. Trost), Pergamon Press, Oxford, U.K., **1991**, Vol. 4, p 517. — [1h] F. J. McQuillin, D. G. N. Parker, R. G. Stephenson, *Transition Metal in Organic Synthesis*, Cambridge, U.K., **1991**. — [1i] M. J. Morris, *Comprehensive Organometallic Chemistry II* (Eds: E. W. Abel, F. G. A. Stone, G. Wilkinson), Pergamon, Oxford, UK, **1994**, Vol. 5, p 471. — [1j] S. G. Davies, T. D. McCarthy, *Comprehensive Organometallic Chemistry II* (Eds: E. W. Abel, F. G. A. Stone, G. Wilkinson), Pergamon, Oxford, UK, **1995**, Vol. 12, p 1039. — [1k] F. Rose-Munch, E. Rose, *Current Org. Chem.* **1999**, 3, 445–467.
- [2] [2a] E. L. Muetterties, J. R. Bleek, E. J. Wucherer, T. A. Albright, *Chem. Rev.* **1982**, 82, 499–525. — [2b] T. A. Albright, P. Hofmann, R. Hoffmann, *J. Am. Chem. Soc.* **1977**, 99, 7546–7557.
- [3] [3a] A. D. Hunter, L. Shilliday, W. S. Furey, M. J. Zaworotko, *Organometallics* **1992**, 11, 1550–1560. — [3b] A. D. Hunter, V. Mozol, S. D. Tsai, *Organometallics* **1992**, 11, 2251–2262.
- [4] J. P. Djukic, F. Rose-Munch, E. Rose, F. Simon, Y. Dromzee, *Organometallics* **1995**, 14, 2027–2038.
- [5] E. P. Kundig, C. Grivet, S. Spichiger, *J. Organomet. Chem.* **1987**, 332, C13–C16.
- [6] [6a] C. A. L. Mahaffy, *J. Organomet. Chem.* **1984**, 262, 33–38. — [6b] C. A. L. Mahaffy, P. L. Pauson, *Inorg. Synth.* **1978**, 21, 136–140.
- [7] [7a] E. L. Eliel, S. H. Wilen, *Stereochemistry of Organic Compounds*, Wiley, New York, **1994**. — [7b] A. Collet, *Comprehensive Supramolecular Chemistry* (Eds: J. L. Atwood, J. E. D. Davies, D. D. MacNicol, F. Vögtle, J. M. Lehn, D. N. Reinhoudt), Pergamon-Elsevier Science, Oxford, U.K., **1996**, Vol. 10, pp 113–149.
- [8] [8a] A. Domenicano, A. Vacagio, C. A. Coulson, *Acta Crystallogr., Sect. B* **1975**, 31, 221–234. — [8b] A. Domenicano, A. Vacagio, C. A. Coulson, *Acta Crystallogr., Sect. B* **1975**, 31, 1630–1641. — [8c] H. Bock, K. Ruppert, C. Näther, Z. Havlas, H.-F. Herrmann, C. Arad, I. Göbel, A. John, J. Meuret, S. Nick, A. Rauschenbach, W. Seitz, T. Vaupel, B. Soulouki, *Angew. Chem. Int. Ed. Engl.* **1992**, 31, 550–581; *Angew. Chem.* **1992**, 104, 564.
- [9] [9a] R. Norrestam, L. Schepper, *Acta Chem. Scand. A* **1981**, 35, 91–103. — [9b] R. Norrestam, L. Schepper, *Acta Chem. Scand. A* **1978**, 32, 889–890. — [9c] T. Maetzke, D. Zeebach, *Helv. Chim. Acta* **1989**, 72, 624–630.
- [10] R. Meyer, M. Schindehutte, P. H. van Rooyen, S. Lotz, *Inorg. Chem.* **1994**, 33, 3605–3608.
- [11] [11a] E. W. Neuse, *J. Organomet. Chem.* **1975**, 99, 287–295. — [11b] T. E. Bitterwolf, *Polyhedron* **1988**, 7, 1377–1382. — [11c] F. van Meurs, J. M. A. Baas, H. van Bekkum, *J. Organomet. Chem.* **1976**, 113, 353–359.
- [12] [12a] J. Y. Saillard, D. Grandjean, F. Chopplin, G. Kaufmann, *J. Mol. Struct.* **1974**, 23, 363–375. — [12b] M. F. Guest, I. H. Hillier, B. R. Higginson, D. R. Lloyd, *Mol. Phys.* **1975**, 29, 113–128.
- [13] D. G. Carroll, S. P. McGlynn, *Inorg. Chem.* **1968**, 7, 1285–1290.
- [14] L. Phillips, C. M. Barnes, M. J. Aroney, *J. Organomet. Chem.* **1997**, 539, 121–125.
- [15] [15a] 6a: Y. Dusaosoy, J. Protas, J. Besançon, J. Tirouflet, C. R. Acad. Sci., Ser. C **1970**, 270, 1792–1794. — [15b] 6b: B. Rees, P. Coppens, *Acta Crystallogr., Sect. B* **1973**, 29, 2515–2528. — [15c] 6c: P. Le Maux, J. Y. Saillard, D. Grandjean, G. Jaouen, *J. Org. Chem.* **1980**, 45, 4524–4526; J. Y. Saillard, D. Grandjean, P. Le Maux, J. Jaouen, *New J. Chem.* **1981**, 5, 153–160. — [15d] 6d: H. J. Wasserman, M. J. Wovkulich, J. D. Atwood, M. R. Churchill, *Inorg. Chem.* **1980**, 19, 2831–2834. — [15e] 6e: F. van Meurs, H. van Konigsveld, *J. Organomet. Chem.* **1977**, 131, 423–428. — [15f] 6f: D. van der Helm, R. A. Loghry, D. J. Hanlon, A. P. Hagen, *Cryst. Struct. Commun.* **1979**, 8, 899. — [15g] 6g: A. Ceccon, G. Giacometti, A. Venzo, G. Zanotti, *J. Organomet. Chem.* **1981**, 205, 61–69. — [15h] 6h: Y. Xiaoguang, H. Jinshun, H. Jinling, *J. Struct. Chem.* **1985**, 4, 52. — [15i] 6k: C. F. Marcos, S. Perrio, A. M. Z. Slawin, S. E. T. Thomas, D. J. Williams, *J. Chem. Soc., Chem. Commun.* **1994**, 753–754. — [15j] 6l: T. J. J. Muller, M. Ansorge, H. J. Lindner, *Chem. Ber.* **1996**, 129, 1433–1440. — [15k] 6m: W. R. Cullen, S. J. Rettig, H. Zhang, *Can. J. Chem.* **1996**, 74, 2167–2181. — [15l] 6n: M. M. Kubicki, P. Richard, B. Gautheron, M. Viotte, S. Toma, M. Hudecek, V. Gajda, *J. Organomet. Chem.* **1994**, 476, 55–62. — [15m] 6o: J. Y. Saillard, D. Grandjean, *Acta Crystallogr., Sect. B* **1976**, 32, 2285–2289. — [15n] 6p–q: T. M. Gilbert, C. B. Bauer, R. D. Rogers, *J. Chem. Crystallogr* **1996**, 26, 355.
- [16] N. Inamoto, S. Masuda, *Chem. Lett.* **1982**, 1003–1006.
- [17] L. Komorowski, S. L. Boyd, R. J. Boyd, *J. Phys. Chem.* **1996**, 100, 3448–3453.
- [18] 7a–h: T. M. Gilbert, A. H. Bond, R. D. Rogers, *J. Organomet. Chem.* **1994**, 479, 73–86.
- [19] 7j: F. Rose-Munch, R. Khourzom, J. P. Djukic, E. Rose, B. Langlois, J. Vaissermann, *J. Organomet. Chem.* **1994**, 470, 131–135.
- [20] 7i: B. R. Jagirdar, K. J. Klabunde, R. Palmer, L. J. Radanovich, T. Williams, *Inorg. Chim. Acta* **1996**, 250, 317–326.
- [21] A. L. Allred, *J. Inorg. Nucl. Chem.* **1961**, 17, 215–221.
- [22] F. Dijkstra, J. H. van Lenthe, *Int. J. Quant. Chem.* **1999**, 74, 213–221.
- [23] C. Hansch, A. Leo, R. W. Taft, *Chem. Rev.* **1991**, 91, 165–195.
- [24] C. Hansch, A. Leo, S. H. Hunger, K. H. Kim, D. Nikaitani, E. Lien, *J. Med. Chem.* **1973**, 16, 1207–1216.
- [25] H. C. Brown, Y. Okamoto, *J. Am. Chem. Soc.* **1958**, 80, 4979–4987.
- [26] F. Kinomura, T. Tamura, I. Watanabe, Y. Yokoyama, S. Ikeda, *Bull. Chem. Soc. Jpn.* **1976**, 49, 3544–3547.
- [27] 7n: F. van Meurs, H. van Konigsveld, *J. Organomet. Chem.* **1974**, 78, 229–235.
- [28] 8a–c: Y. Dusaosoy, J. Protas, J. Besançon, J. Tirouflet, *Acta Crystallogr., Sect. B* **1973**, 29, 469–476.
- [29] 8c: O. L. Carter, A. T. Mc Phail, G. A. Sim., *J. Chem. Soc. A* **1967**, 228–236.
- [30] H. Lumbroso, C. Segard, B. Roques, *J. Organomet. Chem.* **1973**, 61, 249–260.
- [31] L. Farrugia, *ORTEP-3 for Windows, Version 1.03*, Department of Chemistry, University of Glasgow, U.K.
- [32] P. McArdle, *ORTEX for Windows, Version 6*, UCG Crystallography Centre, Chemistry Department, University College Galway, Ireland.
- [33] D. J. Watkin, J. R. Carruthers, P. W. Betteridge, *Crystals User Guide, Chemical Crystallography Laboratory*, University of Oxford, U.K., **1988**.
- [34] *International Table for X-ray Crystallography*, Vol. IV, Kynoch Press, Birmingham, U.K., **1974**.
- [35] G. M. Sheldrick, *SHELXS-86, Program for Crystal Structure Solution*, University of Göttingen, Germany, **1986**.

Received October 19, 1999

[199368]